NOTCH AND DEFECT SENSITIVITY UNDER ANY KIND OF FATIGUE LOADING: AN UNIFYING APPROACH

B. Atzori[1] and L. Susmel[2]
[1]Department of Mechanical Engineering, University of Padova, Padova (Italy)
[2]Department of Engineering, University of Ferrara, Ferrara (Italy)

ABSTRACT

The present paper summarises on an attempt to link together two different engineering tools in order to propose an unifying approach suitable for predicting the material notch- as well as the material defect-sensitivity under multiaxial fatigue loading. The proposed approach takes as its starting point the assumption that the multiaxial fatigue limit of the parent material can initially be predicted by using the Modified Wöhler Curve Method recently proposed by Susmel and Lazzarin [1, 2]. This criterion postulates that the plane of maximum shear stress amplitude is coincident with the micro-crack initiation plane and its application requires the calculation of both the maximum shear stress amplitude and the maximum normal stress relative to the critical plane. According to the unifying diagram proposed by Atzori and Lazzarin [3, 4], the predicted multiaxial plain fatigue limit must then be corrected using both some LEFM concepts and the classical stress concentration factor, K_{tg}. The accuracy of this new approach was checked using a number of data sets taken from the literature and generated testing notched cylindrical bars under in-phase biaxial fatigue loading. The proposed method was successful in estimating notched fatigue limits giving predictions falling within an error interval of ±20%. The introduced schematisation was seen to be a sound engineering method suitable for assessing real components in situations of practical interest.

1 INTRODUCTION

Real mechanical components have complex geometries generating stress concentration phenomena which strongly affect the material fatigue strength. Moreover, in service loadings are, in general, multiaxial and it is well-know that the classical equivalent stresses (for instance, Von Mises, Tresca, Beltrami, etc.) are not successful in predicting the multiaxial fatigue strength, and it holds especially true in the presence of out-of-phase loading. Therefore, it is evident that engineers engaged in assessing real components need simple tools to address this complex problem.

Recently, Atzori et al. [3, 4] proposed a unifying diagram (fig. 1) suitable for predicting the defect- as well as the notch-sensitivity under uniaxial fatigue loading. This diagram has in the abscissa the notch depth, a, and in the ordinate the notched fatigue limit referred to the gross area, $\Delta\sigma_g$. Initially, this approach was proposed just for a crack in an infinite plate [3], but, subsequently, the same authors extended the validity of this diagram to real components [4]. Figure 1 shows that the fatigue limit reduction due to different kind of stress concentrators can be schematised using three straight lines: the upper limit is given by the material plain fatigue limit, $\Delta\sigma_0$; the intermediate zone is described by the classical LEFM equation, accounting for the geometry of the assessed component by the shape factor α; finally, the lower limit can be calculated according to the classical stress-life method: $\Delta\sigma_g=\Delta\sigma_0/K_{tg}$. The two transition points subdividing Atzori-Lazzarin's diagram into three different areas turn out to be [4]:

$$a_D = \frac{a_0}{\alpha^2} \tag{1}$$

$$a_N = \frac{K_{tg}^2 \cdot a_0}{\alpha^2} \tag{2}$$

where $a_0=1/\pi(\Delta K_{th}/\Delta\sigma_0)^2$ [5].

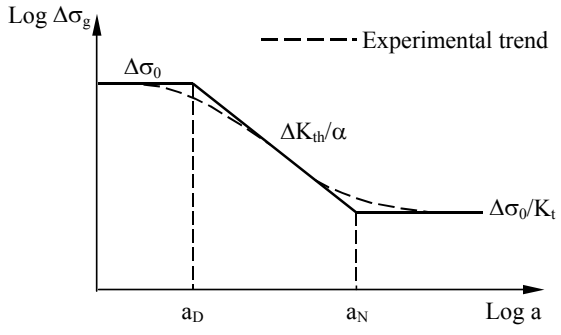

Figure 1: Atzori-Lazzarin diagram.

Recently, Susmel and Lazzarin [1, 2] proposed a new criterion to predict the parent material fatigue limit under multiaxial fatigue loading. This criterion is based on the assumption that the plane experiencing the maximum shear stress amplitude, τ_a, is the one on which the probability of having the crack initiation reaches its maximum value. Moreover, fatigue damage depends also on the maximum stress, $\sigma_{n,max}$, perpendicular to the critical plane (according to Socie's fatigue damage model). The combined effect of these two stress components can simultaneously be accounted for by the stress ratio relative to the assumed crack initiation plane [1]:

$$\rho = \frac{\sigma_{n,max}}{\tau_a}. \tag{3}$$

This stress parameter was seen to be sensitive both to non-zero out-of-phase angles and to non-zero mean stresses. Moreover, it is trivial to demonstrate that under fully-reversed uniaxial fatigue loading ρ is equal to unity, whereas under fully-reversed torsional loading it equals zero [1]. The material fatigue behaviour can be depicted in a Modified Wöhler Diagram (fig. 2a): as the ρ value changes different curves are generated and these curves move downward as ρ increases. Assuming a linear relationship between the maximum shear stress amplitude and ρ, the Modified Wöhler Curve Method can be formalised as follows [1]:

$$\tau_a \le \tau_A(\rho) = \left(\frac{\sigma_0}{2} - \tau_0\right)\cdot\rho + \tau_0, \tag{4}$$

where σ_0 and τ_0 are the fully-reversed plain uniaxial and torsional fatigue limit, respectively: when $\tau_a=\tau_A(\rho)$, the studied material is in fatigue limit condition.

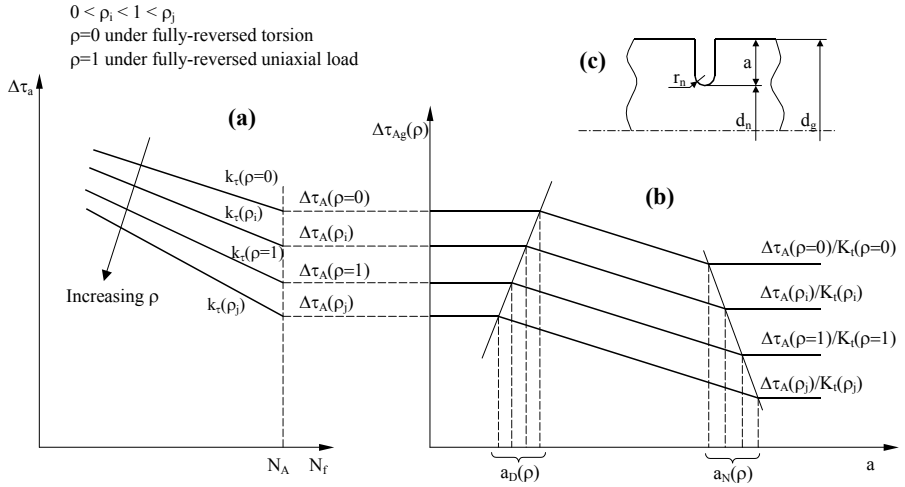

Figure 2: Link between the Modified Wöhler diagram and the Atzori-Lazzarin diagram.

This criterion was seen to be very accurate in predicting the multiaxial fatigue limit of smooth components independently of both material and applied loading type [1, 2]. Moreover, it can be remembered here that this approach demonstrated to be successful in predicting also the multiaxial fatigue limit of bluntly notched components, when predictions are performed in terms of nominal net stresses and the plain fatigue limits are corrected by using a generalisation of the classical strength reduction factor, K_f [2]. This aspect will be discussed in more detail below.

2 THE NEW METHOD FRAME

Initially, to formalise the new method, consider a U-notched cylindrical bar subjected to an uniaxial fatigue loading (fig. 2c). In the Modified Wöhler Diagram (fig. 2a), the curve under uniaxial fatigue loading is characterised by a ρ value equal to 1. Now the Atzori-Lazzarin diagram can easily be re-plotted in terms of maximum shear stress range calculated with respect to the gross area (fig. 2b). The upper and the lower limit are given by $\Delta\tau_A(\rho=1)= \Delta\sigma_0/2$ and by $\Delta\tau_A(\rho=1)/K_{tg}(\rho=1)$, respectively, where $K_{tg}(\rho=1)$ is the value of the stress concentration factor under uniaxial loading. The sloping straight line joining these two limits can easily be derived by dividing by 2 the notch fatigue limit values given by the classic LEFM equation.

Now the same procedure can be applied to build the Atzori-Lazzarin curve under fully-reversed torsional fatigue loading (ρ=0). The upper and the lower limit must be calculated, respectively, as: $\Delta\tau_A(\rho=0)= \Delta\tau_0$ and $\Delta\tau_A(\rho=0)/K_{tg}(\rho=0)$, where $K_{tg}(\rho=0)$ is the value of the stress concentration factor under torsion. It is logical now to form the hypothesis that as ρ changes different curves are generated in the Atzori-Lazzarin diagram, provided that, it is reinterpreted in terms of maximum shear stress range (fig. 2b). In particular, according to the Modified Wöhler Curve Method, these curves are supposed to move downward as the ρ ratio increases.

Consider now an Atzori-Lazzarin curve to be determined for a generic ρ value. Initially, the corresponding plain fatigue limit can be estimated by eqn (4). Subsequently, the position of the transition point $a_D(\rho)$ must be determined. According to eqns (1) and (2), the value of this point depends on a_0. In the present paper, as suggested by Susmel in Ref. [6], a_0 is assumed to be a material constant and its reference value must be determined under fully-reversed uniaxial fatigue loading. If $\alpha(\rho=1)$ and $\alpha(\rho=0)$ are the shape factor values under uniaxial and torsional loading, respectively, the value of $\alpha(\rho)$ and $a_D(\rho)$ could be calculated by the following relationships:

$$\alpha(\rho) = \left[\alpha(\rho=1) - \alpha(\rho=0)\right]\cdot\rho + \alpha(\rho=0) \quad (5)$$

$$a_D(\rho) = \left[a_D(\rho=1) - a_D(\rho=0)\right]\cdot\rho + a_D(\rho=0)\,. \quad (6)$$

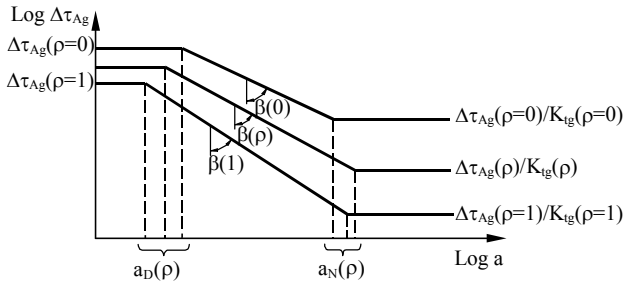

Figure 3: Generalised Atzori-Lazzarin diagram.

The previous equations were obtained assuming a linear relationship between $\alpha(\rho)$ and ρ as well as between $a_D(\rho)$ and ρ, as done by Susmel and Lazzarin to determine eqn (4).

The sloping part of the generic Atzori-Lazzarin curve can be described using to the following equation:

$$\Delta K_{th}(\rho) = \alpha(\rho)\cdot\Delta\tau_{Ag}(\rho)\cdot\sqrt{\pi}\cdot a^{\beta(\rho)} \quad (7)$$

Eqn (7) represents a generalisation to multiaxial fatigue situations of the classic LEFM stress intensity factor vs. fatigue limit relationship. In particular, in eqn (7) $\Delta K_{th}(\rho)$ is a generalised SIF, $\alpha(\rho)$ is the generalised shape factor given by eqn (5), $\Delta\tau_{Ag}(\rho)$ is the unknown fatigue limit relative to the critical plane, a is the notch depth and, finally, $\beta(\rho)$ is an exponent depending on Williams' eigenvalues [6]. From a practical point of view, eqn (7) can easily be determined as an exponential equation passing through the point having coordinates $[\Delta\tau_A(\rho), a_D(\rho)]$.

Particular attention must be paid to the calculation of $\beta(\rho)$. It is common opinion that the eigenvalues under mode I loading does not change significantly as long as the notch opening angle is less than 90° (see Tab. 1). On the contrary, the value of β under mode III loading, that is, under anti-plane stress, is strongly affected by the opening angle value, as shown by Table 1. This means that for open notches the slope of the sloping part of the Atzori-Lazzarin curve changes as the ρ value changes.

Table 1: Williams' exponents under uniaxial (ρ=1) and torsional loading (ρ=0)

Opening Angle	0°	30°	90°	135°
$\beta(\rho=1)$	0.500	0.499	0.456	0.326
$\beta(\rho=0)$	0.500	0.454	0.333	0.200

This situation is sketched in figure 3, where the Atzori-Lazzarin diagram has been built considering a cylindrical bar weakened by a circumferential V-notch having an opening angle value approaching 90°. Assuming again a β vs. ρ linear relationship, the exponent of eqn (7) can then be expressed as:

$$\beta(\rho) = [\beta(\rho=1) - \beta(\rho=0)]\cdot\rho + \beta(\rho=0)\,. \tag{8}$$

Lastly, the lower limit of the generic Atzori-Lazzarin curve can be determined observing that Lazzarin and Susmel in Ref. [2] introduced a generalisation to multiaxial fatigue situations of the classical fatigue strength reduction factor. By using a large database of fatigue data, they verified that the multiaxial K_{fg} can easily be expressed as:

$$K_{fg}(\rho) = \left[K_{fg}(\rho=1) - K_{fg}(\rho=0)\right]\cdot\rho + K_{fg}(\rho=0)\,. \tag{9}$$

Under uniaxial fatigue loading, when a notched component is in full notch sensitivity condition, the following identity can be written: $K_{tg}(\rho=1)=K_{fg}(\rho=1)$. It is trivial now to generalise this assumption under any kind of fatigue loading by using eqn (9):

$$K_{tg}(\rho) = \left[K_{tg}(\rho=1) - K_{tg}(\rho=0)\right]\cdot\rho + K_{tg}(\rho=0)\,. \tag{10}$$

According to the previous considerations, the position of the lower limit of the generic Atzori-Lazzarin curve can be calculated as:

$$\Delta\tau_{Ag} = \frac{\Delta\tau_A(\rho)}{K_t(\rho)} \tag{11}$$

Finally, the value of $a_N(\rho)$ turns out to be:

$$a_N(\rho) = a_0\left[\frac{K_{tg}(\rho)}{\alpha(\rho)}\right]^{\frac{1}{\beta(\rho)}} \tag{12}$$

3 METHOD VALIDATION BY EXPERIMENTAL DATA

The accuracy of the proposed method was checked by using some data taken from the technical literature. These data were generated testing cylindrical V-notched bars under biaxial in-phase

fatigue loading. In figure 4, the geometries of the considered specimens are sketched, whereas Table 1 summarises the main pieces of information on the data considered in this study.

Table 2: Summary of the experimental data generated under multiaxial fatigue loadings.

Material	Ref.	$\Delta\sigma_0$ [MPa]	$\Delta\tau_0$ [MPa]	σ_{UTS} [MPa]	K_{tg} ρ=1	K_{tg} ρ=0	a_0 [6] [mm]	α [10] ρ=1	α [10] ρ=0	Applied loads*	N. of Series
0.4% C steel (norm.)	[8]	663.8	413.8	648.4	26.2	12.5	0.111	1.23	1.14	B-T	5
3% Ni steel	[8]	685.4	410.6	526.4	26.2	12.5	0.145	1.23	1.14	B-T	5
Cr-Va steel	[8]	858.2	515.6	751.8	17.6	9.0	0.100	1.23	1.14	B-T	5
3.5% NiCr (N-I)	[8]	1080.6	704.0	895.3	12.7	6.8	0.103	1.23	1.14	B-T	5
3.5% NiCr steel (L-I)	[8]	1018.8	648.4	896.9	12.7	6.8	0.098	1.23	1.14	B-T	5
NiCrMo (75-80 tons)	[8]	1321.4	685.4	1242.7	10.9	6.1	0.075	1.23	1.14	B-T	5
LCS (r_n=0.4mm)	[9]	424.0	353.8	500.0	15.7	8.8	0.143	2.10	2.07	PP-T	3
LCS (r_n=0.2mm)	[9]				21.3	11.1		2.10	2.07	PP-T	3

*B=bending; PP=push-pull; T=torsion.

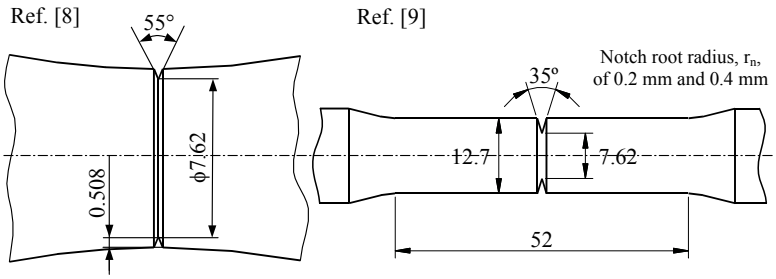

Figure 4: Specimen geometries (Dimensions in millimetres).

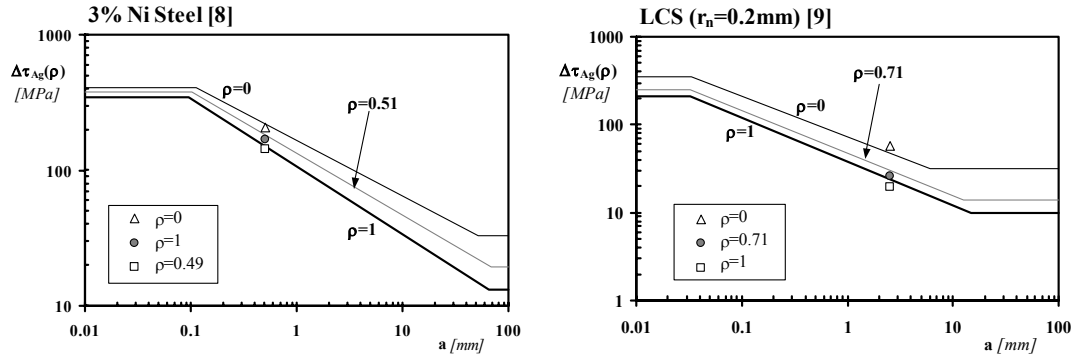

Figure 5: Generalised Atzori-Lazzarin diagrams and experimental data (experimental fatigue limits extrapolated at 10^7 cycles to failure).

In particular, it is important to highlight here that, due to the lack of information, a_0 values were determined in Ref. [6] by comparing the uniaxial plain to the notched fatigue limit both extrapolated at 10^7 cycles to failure. The correct definition of a_0 would have required the real material plain fatigue limit (evaluated by using, for instance, the Stair Case method) and the range of the threshold value of the stress intensity factor, both determined under R = –1.

As example, in figure 5 the generalised Atzori-Lazzarin diagrams have been reported for two different materials. Moreover, to be as clear as possible, only three points for every considered material have been plotted: the notch fatigue limit under fully-reversed uniaxial fatigue loading (ρ=1), under fully-reversed torsional fatigue loading (ρ=0) and, finally, an intermediate case. These diagrams show the sound agreement between the proposed method and the experimental results. Finally, in figure 6 the experimental, τ_{Ag}, vs. the estimated fatigue limit, $\tau_{Ag,e}$, diagram for all the considered data series is reported.

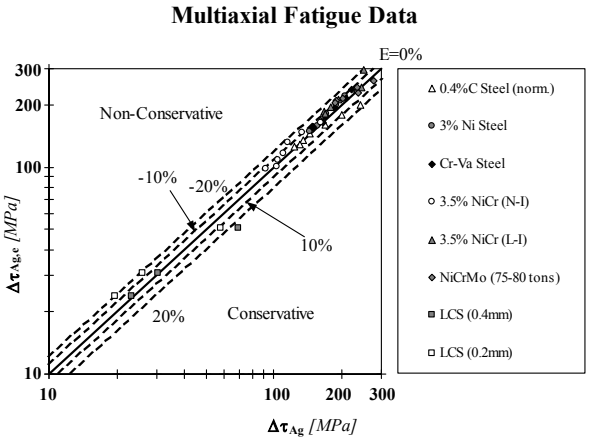

Figure 6: Experimental, τ_{Ag}, vs. predicted, $\tau_{Ag,e}$, fatigue limit diagram.

This diagram demonstrates that our method is capable of predictions laying within an error interval of ±20%, independently of material and ratio between the applied uniaxial and torsional stress.

4 CONCLUSIONS

The proposed method demonstrated to be a powerful tool suitable for predicting, in terms of nominal stresses, the fatigue limit of notched components independently of notch feature and degree of multiaxility of the applied load, joining the defect- to the notch-sensitivity regime under any kind of fatigue loading.

REFERENCES

[1] Susmel L., Lazzarin P., A Bi-Parametric Modified Wöhler Curve for High Cycle Multiaxial Fatigue Assessment. Fatigue Fract. Engng. Mater. Struct., Vol. 25, pp. 63-78, 2002.

[2] Lazzarin P., Susmel L., A Stress-Based Method to Predict Lifetime under Multiaxial Fatigue Loadings. Fatigue Fract. Engng. Mater. Struct 26, pp. 1171-1187, 2003.

[3] Atzori, B., Lazzarin, P. Notch sensitivity and defect sensitivity under fatigue loading: two sides of the same medal. Int. J. Fracture, 107, L3-L8, 2000.

[4] Atzori B., Lazzarin P., Meneghetti G., Fracture mechanics and notch sensitivity. Fatigue Fract. Engng. Mater. Struct. 26 3, 257-268, 2003.

[5] Taylor, D., Geometrical effects in fatigue: a unifying theoretical model. Int. J. Fatigue, 21, pp. 413-420, 1999.

[6] Susmel L., A unifying approach to estimate the high-cycle fatigue strength of notched components subjected to both uniaxial and multiaxial cyclic loadings. Fatigue Fract. Engng. Mater. Struct., 2004, in press.

[7] Williams M. L., Stress singularities resulting from various boundary conditions in angular corners of plates in extension, J. Appl. Mechanics, 19, pp. 526-528, 1952.

[8] Gough H. J., Engineering Steels under Combined Cyclic and Static Stresses. In: Proc. Inst. Mech. Engrs. 160, pp.417-440, 1949.

[9] Quilafku G. et al., Fatigue of Specimens Subjected to Combined Loading. The Role of hydrostatic pressure. Int. J. Fatigue 23, pp. 689-701, 2001.

[10] Tada H., Paris P.C., Irwing G.R., The Stress Analysis of Cracks – Handbook. Professional Engineering Publishing, Bury St. Edmunds, UK, 2000 (Third Edition).